

The effect of thiol collectors on nickel-rich (110) pentlandite surface using density functional theory

P P Mkhonto¹, H R Chauke¹ and P E Ngoepe¹

¹ Materials Modelling Centre, University of Limpopo, Private Bag x1106, Sovenga, 0727, South Africa

E-mail: peace.mkhonto@ul.ac.za, peace.mkhonto@gmail.com

Abstract. *Ab-initio* density functional theory was employed to investigate the interaction of thiol collectors on the nickel-rich pentlandite ($\text{Fe}_4\text{Ni}_5\text{S}_8$) (110) surface, in order to establish an insight into the collecting performances of SEX, SIBX and DEDTP collectors during flotation. The HOMO and LUMO energies of the three collectors were computed from DMol³ and revealed that SIBX had the strongest ability to donate electrons, while di-Et-DTP accept electrons. Furthermore, the collecting strength of di-Et-DTP on the nickel-rich pentlandite mineral (110) surface is mostly preferred amongst the three collectors. In addition, we observed that the Fe atoms had the strongest adsorption than Ni atoms.

1. Introduction

Nickel mining is popular in over 20 countries including South Africa, contributing in various industrial applications such as stainless steel, coins and rechargeable batteries; as such the demand for nickel is ever growing [1]. Pentlandite, in particular $(\text{Fe}, \text{Ni})_9\text{S}_8$ is a principal source of nickel [2], however the mineral occurs as intergrowth or in solid solution with pyrrhotite [3] and this makes extraction of mineral difficult. The separation of minerals can be achieved by stage-adding of organic collectors which form important role in rendering the mineral hydrophobic. The collector attach through its polar sulphur atoms to only valuable mineral particles so that water is repelled thus creating a favourable condition for the desired mineral particles to adhere to air bubbles upon collision [4]. As such the air bubbles carry the hydrophobic material (concentrates) to the pulp surface.

Although performing flotation using xanthate collectors is still a challenge, the xanthate collectors are known as low-cost, easy-to-produce collectors which usually give good flotation efficiency. The dithiophosphate are also used but were found not suitable to replace the xanthate on the flotation of pentlandite containing ore [5]. However, the dithiophosphate was found to increase the selectivity during the floatation of pentlandite when it is used as a co-collector with xanthate during flotation [6–8]. Interestingly, the mixture of SIBX and DTP collectors was shown previously to increase the recovery of nickel grades. The increase in cumulative recoveries of nickel indicated the recovery of the pentlandite [8].

In this paper, we employ first principles method to investigate the surface properties of nickel-rich pentlandite mineral, starting from the surface orientation and termination to better understand the surface reaction with SEX, SIBX and di-Et-DTP collectors. Importantly, the interaction of collectors with pentlandite during floatation is an important process to understand extraction of

mineral ore. This investigation will provides information on the collector interaction with pentlandite (110) surfaces that may be applicable to the separation of pentlandite mineral.

2. Computational methodology

In order to investigate the interaction of collectors on (110) surface of nickel-rich pentlandite mineral, we perform *ab initio* quantum-mechanical density functional theory calculations [9, 10], and analyze the density of states and Bader analysis. We use the plane-wave (PW) pseudopotential method with Perdew-Burke-Ernzerhof (PBE) exchange-correlation functional [9], using VASP code [12]. A (110) surface slab composed of four layers before relaxation and six layers after relaxation separated by a vacuum slab of 20 Å was used to mimic the interaction of the adsorbate with the repeating upper slab. The ultrasoft pseudopotential is used with a plane-wave basis set, truncated at cut-off energy of 400 eV since this was found to be sufficient to converge the total energy of the system. Brillouin zone integrations are performed on a grid of 5x5x1 k-points. This is chosen according to the scheme proposed by Monkhorst and Pack [13]. Different termination were sampled and only the less reactive (low surface energy) for (110) surfaces were considered. The surface stabilities for different termination are determined by their surface energy, calculated using equation 1:

$$E_{\text{surface}} = \left(\frac{1}{2A}\right) [E_{\text{slab}} - (n_{\text{slab}})E_{\text{bulk}}] \quad (1)$$

where E_{slab} is the total energy of the cell containing the surface slab, n_{slab} is the number of atoms in the slab, E_{bulk} is the total energy per atom of the bulk and A is the surface area. A low positive value of E_{surface} indicates stability of the surface termination. During adsorption the bottom two layers are kept frozen and the top four layers are allowed to interact with the oxygen molecule. The interaction strength of the surface with the adsorbate is shown by the adsorption energy, calculated by equation 2:

$$E_{\text{adsorption}} = [E_{\text{system}} - (E_{\text{slab}} + E_{\text{collector}})] \quad (2)$$

where E_{system} is the energy of the surface slab with collector, E_{slab} is the energy of the surface slab and $E_{\text{collector}}$ is the energy of the isolated collector molecule. A negative value shows a strong interaction between the adsorbate and the surface, whereas a positive value reveals the opposite.

Now, in order to calculate reaction energies, the optimization of SEX, SIBX and di-Et-DTP were calculated in a cubic cell of $a = 25$ Å using the same organic collectors, PAW potential, cut-off energy and other precision parameters as in the surface calculations. Further geometry optimizations of the collectors were performed with DMol³ [14] to calculate the highest occupied molecular orbital (HOMO) and lowest un-occupied molecular orbital (LUMO) energies. These were performed using GGA-PBE functional. The double numerical plus polarisation (DNP) basis set with 4.4 Basis file was set using the DFT Semi-core Pseudopotentials, with other parameters at medium settings. The charge states of the ions at the surface were discussed on the basis of a Bader analysis, which consists of integrating the electron density in a region defined for each atom in such a way that the density gradient flux through the dividing surfaces is zero [15]. An algorithm and a program developed for this purpose by Henkelman *et al.* have been employed [16, 17].

3. Results and discussion

The nickel-rich pentlandite ($\text{Fe}_4\text{Ni}_5\text{S}_8$) (110) surface is shown in figure 1, and the designated atoms as indicated. The surface was cleaved from the optimised bulk pentlandite structure in figure 1a with space group of *Fm-3m* (225) [18]. Their calculated surface and adsorption energies are given in table 1.

Table 1. Calculated surface energy ($\text{eV}/\text{\AA}^2$) and adsorption energies (eV) of organic collectors adsorbed on (110) nickel-rich pentlandite mineral surface metals.

Surface	Surface energy		Adsorption energies				
	E_{surface}	SEX	SIBX		di-Et-DTP		
(110)	0.122	Ni	Fe	Ni	Fe	Ni	Fe
		-0.884	-1.984	-0.999	-2.126	-1.266	-2.916

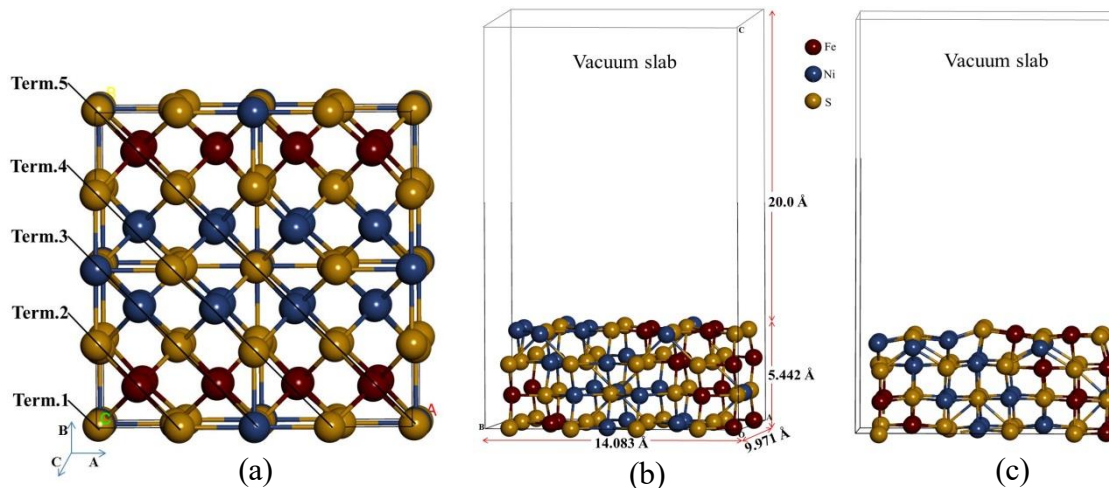


Figure 1: The $\text{Fe}_4\text{Ni}_5\text{S}_8$ pentlandite structures: (a) Conventional bulk structure showing different terminations, (b) (110) surface un-relaxed Term.3 and (c) relaxed stable term.3 surface.

Note that the bonding behavior and charge state of the clean pentlandite surface was discussed from the density of states (DOS) and Bader analysis in our previous work [19], where the DOS showed a metallic characteristic behavior since there was no energy band gap (E_g) observed at the Fermi energy (E_F).

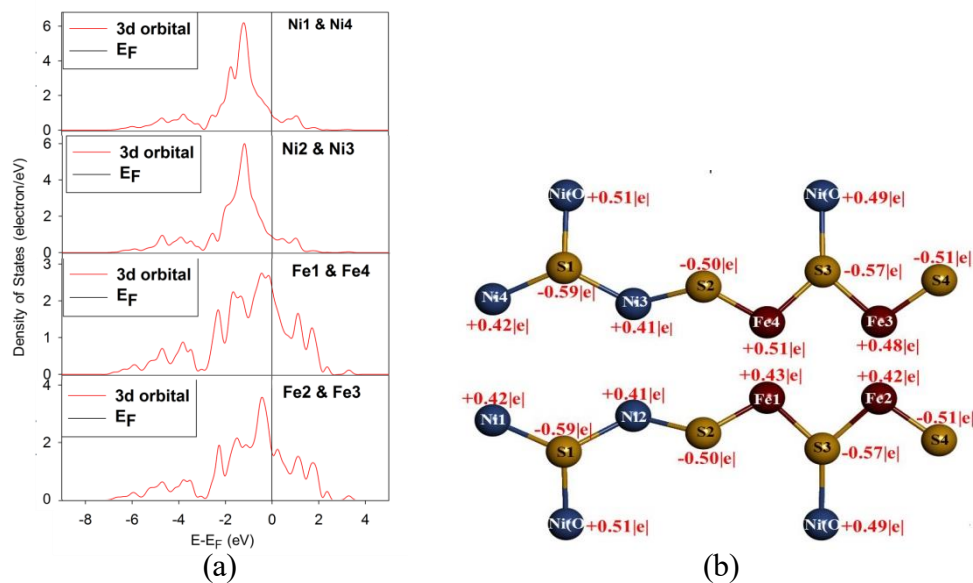


Figure 2: The $\text{Fe}_4\text{Ni}_5\text{S}_8$ pentlandite (110) surface: (a) Top Fe and Ni atoms partial density of states and (b) Bader charges for the top layer atoms.

The PDOS of Ni atoms showed only one sharp peak at the VB and less contribution at E_F , while the PDOS of Fe had broader peaks around E_F . More importantly, we noted that the E_F cuts the top of Fe 3d-orbital (high states at E_F) as shown in figure 2a. The surface relaxation had been discussed previously and we observed that the clean iron atoms were observed to have different charges. This suggested that the iron atoms are not charge ordered and there is alternation of the charges on the iron atoms (figure 2b) [19]. Now, the HOMO-LUMO energies could be significant to describe the electronic behaviour of thiol collectors prior to adsorption on the surface.

Table 2. Calculated HOMO and LUMO Energies (eV) for SEX, SIBX and di-Et-DTP, DMol³.

	SEX	SIBX	di-Et-DTP
HOMO	-4.677	-4.674	-5.690
LUMO	-1.423	-1.420	-4.834
H-L gap	3.254	3.254	0.856

From the HOMO and LUMO energies calculated using DMol³ we determined the gap between the HOMO-LUMO (H-L gap) shown in table 2. It has been reported that the molecule with the highest HOMO energy has the strongest ability to donate its electrons to the mineral surface and a molecule with the lowest LUMO energy has the strongest ability to accept electrons from the mineral surface [20]. Based on this report our calculated HOMO and LUMO energies indicates the order of electron donating as: SIBX > SEX > di-Et-DTP and the order of accepting electrons as: di-Et-DTP > SEX > SIBX. Thus the SIBX has the strongest electron donating while the di-Et-DTP has the strongest accepting ability. This is in accordance with the H-L gap, the smaller gap is observed for di-Et-DTP which indicates stronger interaction amongst the collectors and the order of reactivity followed as Et-DTP > SIBX = SEX.

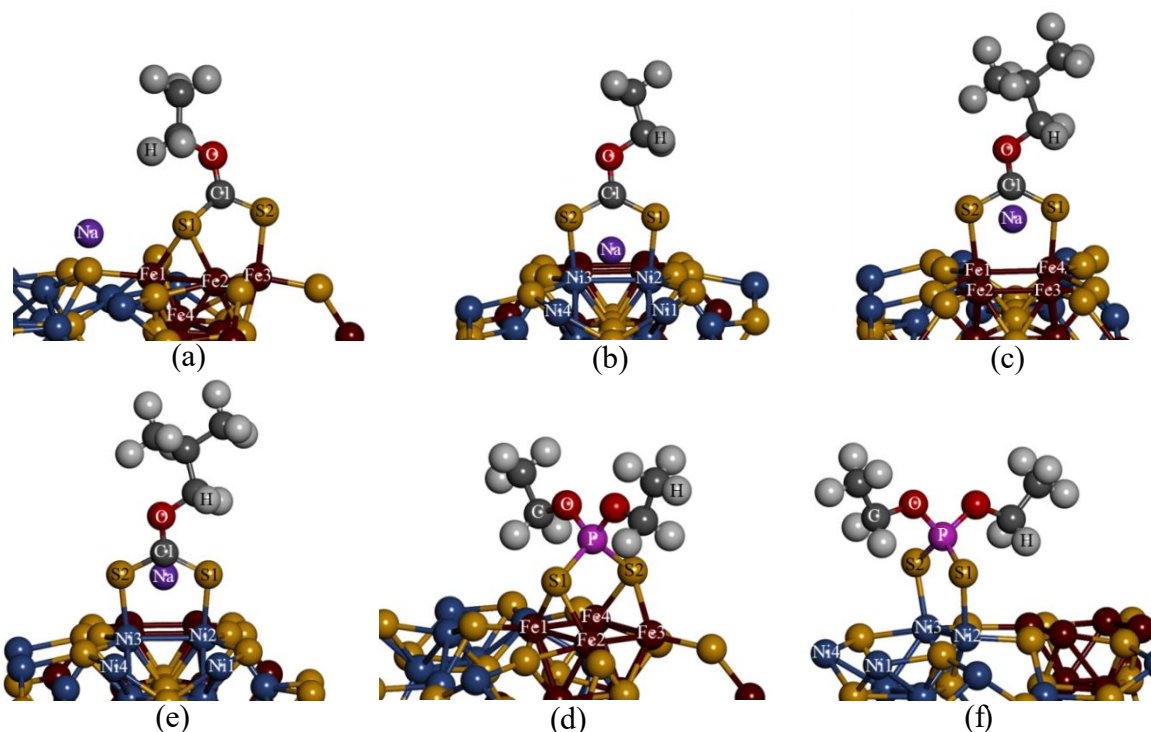


Figure 3: The geometries of xanthate and DTP adsorption on $Fe_4Ni_5S_8$ (110) surface: (a) SEX on Fe-top, (b) SEX on Ni-top, (c) SIBX on Fe-top, (d) SIBX on Ni-top, (e) di-Et-DTP on Fe-top and (f) di-Et-DTP on Ni-top.

In order to ascertain the adsorption of SEX, SIBX and di-Et-DTP on the surface, we considered the most active sites, the Ni-top and Fe-top adsorption sites. Now, when adsorbing on the nickel, we observed that the collectors adsorb and move the nickel atoms back to the upper most layer. Interestingly, we observed that SEX and di-Et-DTP ligand prefer to bridge bond on the iron atoms with the collector sulphur atoms, forming a tripodal and tetrapodal geometry, respectively (figure 3). We also observed that the di-Et-DTP is more favourable and the adsorption energies followed the order as: di-Et-DTP > SIBX > SEX for both Ni-top and Fe-top sites as shown in table 1. A clear increasing trend in adsorption energy from SEX to di-Et-DTP for both Ni-top and Fe-top was observed, which is in agreement with the H-L gap prediction. It is evident that the adsorption energy on Fe is more spontaneous than on Ni site.

4. Conclusions

The adsorption and bonding nature of SEX, SIBX and di-Et-DTP on the (110) surface were described from adsorption energies and electronic structures DFT calculations. An insight on the effect and how flotation process could be enhanced through use of thiol collectors was established. We observed that the di-Et-DTP had the strongest adsorption and more spontaneous on Fe atoms than Ni atoms. Furthermore, we observed that SEX and di-Et-DTP prefer to form a tripodal and tetrapodal geometry on the surface, respectively. These findings suggest that the use of SIBX as collector and di-Et-DTP as co-collector may improve the floatability of the pentlandite. This investigation provides information on the adsorption mechanism strength of xanthates on pentlandite (110) surfaces that may be applicable to the separation of pentlandite mineral.

Acknowledgements

The calculations were performed at the Materials Modelling Centre (MMC), University of Limpopo. We acknowledge the Centre for High Performance Computing (CHPC) for computing resources, the Department of Science and Technology (DST) and South African Mineral to Metals Research Institute (SAMMRI) for financial support.

References

- [1] Ngobeni W A and Hangone G 2013 The effect of using sodium di-methyl-dithiocarbamate as a co-collector with xanthates in the froth flotation of pentlandite containing ore from Nkomati mine in South Africa. *Miner. Eng.* **54** 94–99
- [2] Borodaev Yu, Bryzgalov S I A, Mozgova N N and Uspenskaya T 2007 Pentlandite and Co-Enriched Pentlandite as Characteristic Minerals of Modern Hydrothermal Sulfide Mounds Hosted by Serpentinized Ultramafic Rocks (Mid-Atlantic Ridge). *Vestnik Moskovsk Universiteta. Geologiya* **62** 85–97
- [3] Rajamani V and Prewitt C T 1973 Crystal chemistry of natural pentlandites. *Can. Mineral.* **12** 178–187
- [4] www.jmeech.mining.ubc.ca/MINE290/Froth%20Flotation.pdf. (2012, october 20)
- [5] Ngobeni W and Hangone G 2013 The effect of using pure thiol collectors on the froth flotation of pentlandite containing ore. *South Africa. J. Chem. Eng.* **18** 41–50
- [6] Bradshaw D J, Buswell A M, Harris P J and Ekmekci Z 2005a Interactive effect of the type of milling media and copper sulphide addition on the flotation performance of sulphide minerals from Meresky ore part 1: pulp chemistry. *Int. J. Miner. Process.* **78** 164–174
- [7] Nashwa V M 2007 *The flotation of high talc-containing ore from the great Dyke of Zimbabwe*. Pretoria, South Africa: University of Pretoria
- [8] Nyambayo C K 2014 *The use of mixed thiol collectors in the flotation of Nkomati sulphide ore*. Cape Town, South Africa: University of Cape Town
- [9] Hohenberg P and Kohn W 1965 Inhomogeneous electron gas. *Phys. Rev. B* **136** 864–871
- [10] Kohn W and Sham L J 1965 Self-consistent equations including exchange and correlation effects. *Phys. Rev.* **140** 1133–38

- [11] Perdew J P, Burke K and Ernzerhof M 1996 Hybrid functionals based on a screened coulomb potential. *J. Chem. Phys.* **118** 8207–15
- [12] Kresse G and Furthmüller J 1996 Efficient iterative schemes for ab-initio total-energy calculations using a plane-wave basis set. *Phys. Rev. B* **54** 11169–186
- [13] Monkhorst H F and Park J D 1976 Special points for Brillouin-Zone integrations. *Phys. Rev. B* **13** 5188–92
- [14] Delley B 2000 Density Functional Theory Electronic Structure Program. *J. Chem. Phys.* **113**, 7756
- [15] Bader R F W *Atoms in Molecules: A Quantum Theory*, Oxford University Press: London, UK, 1994
- [16] Sanville E, Kenny S D, Smith R and Henkelman G 2007 An improved grid-based algorithm for Bader charge allocation. *J. Comput. Chem.* **28** 899–908
- [17] Henkelman G, Arnaldsson A and Jonsson H 2006 A fast and robust algorithm for Bader decomposition of charge density. *Comput. Mater. Sci.* **36** 354–360
- [18] Geller S 1962 Refinement of the crystal structure of Co₉S₈. *Acta Crystallogra.* **15** 1195–98
- [19] Mkhonto P P, Chauke H R and Ngoepe P E 2015 Ab initio studies of O₂ adsorption on (110) nickel-rich pentlandite (Fe₄Ni₅S₈) mineral surface. *Miner.* **5** 665–678
- [20] Liu G, Wang Y, Yuan L, Xu Z, Lu Y, Zeng H and Zhong H 2012 A DFT study on the flotation performance of thiol collectors for copper sulphide flotation. *xxvi International Minerals Processing Congress (IMPC)* 02947–02958 New Delhi India